

Entanglement-assisted quantum feedback control *

Naoki Yamamoto and Tomoaki Mikami

Department of Applied Physics and Physico-Informatics, Keio University,
Hiyoshi 3-14-1, Kohoku, Yokohama 223-8522, Japan

January 28, 2022

Abstract

The main advantage of quantum metrology relies on the effective use of entanglement, which indeed allows us to achieve strictly better estimation performance over the standard quantum limit. In this paper, we propose an analogous method utilizing entanglement for the purpose of feedback control. The system considered is a general linear dynamical quantum system, where the control goal can be systematically formulated as a linear quadratic Gaussian control problem based on the quantum Kalman filtering method; in this setting, an entangled input probe field is effectively used to reduce the estimation error and accordingly the control cost function. In particular, we show that, in the problem of cooling an opto-mechanical oscillator, the entanglement-assisted feedback control can lower the stationary occupation number of the oscillator below the limit attainable by the controller with a coherent probe field and furthermore beats the controller with an optimized squeezed probe field.

1 Introduction

Entanglement is a special notion that had been considered as a “spooky” correlation [1]. However over recent decades it has gained a positive impression mainly thanks to its central role in quantum information science [2, 3]. A particularly important application of entanglement in our context is the *quantum metrology* [4, 5]. The basic configuration is depicted in Fig. 1. The goal is to estimate an unknown parameter ϑ of the system. A standard estimation method is first to send a known input state and then measure the output state containing the information about ϑ (Fig. 1 (a)); in this case the estimation error has a strict lower bound called the *standard quantum limit (SQL)* with respect to the input energy. In the quantum metrology schematic depicted in Fig. 1 (b), on the other hand, an entangled state is chosen as an input so that one portion passes through the system while the other portion does not; then by measuring the combined output, we obtain more information about ϑ than the standard case (Fig. 1 (a)) and thus can beat the SQL in the estimation error. This schematic have been experimentally demonstrated in several settings, e.g., [6, 7, 8, 9]. Note that the entanglement-assisted method is not a unique approach for beating the SQL; particularly in the case where ϑ is the parameter of a force applied to a mechanical oscillator (e.g., a gravitational wave force), several alternative estimation schemes beating the SQL have been developed, such as the squeezed-probe scheme [10, 11, 12, 13] and the variational measurement technique [14] for back-action evasion.

What we learn from the theory of quantum metrology is the fact that, in a broad sense, a quantum estimator could have better performance if assisted by entanglement. Therefore it is a reasonable idea to employ an entanglement-assisted estimation strategy for the measurement-based quantum feedback control [15, 16], which is now well established based on the quantum filtering theory [17, 18]. Actually, in a

*This work was supported in part by JSPS Grant-in-Aid No. 15K06151 and JST PRESTO No. JPMJPR166A. The authors acknowledge helpful discussions with M. R. Hush, A. R. R. Carvalho, and S. S. Szigeti.

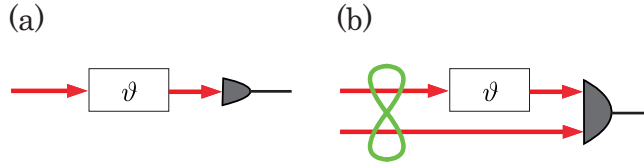


Figure 1: (a) Standard setup for estimating an unknown parameter ϑ . (b) Quantum metrology setup using an entangled input.

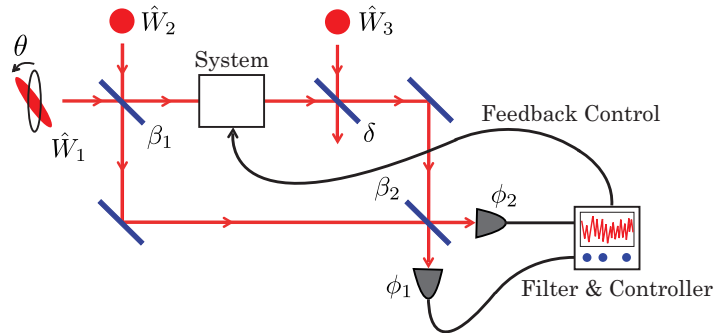


Figure 2: General feedback control configuration via an entangled input field. \hat{W}_1, \hat{W}_2 are field annihilation operators representing a squeezed state with phase θ and a coherent (or vacuum) state, respectively. \hat{W}_3 represents a vacuum field. β_1^2, β_2^2 , and δ^2 denote the reflectivity of the beam splitters; in particular δ corresponds to an optical loss of the system's output field. ϕ_1 and ϕ_2 are the phases of Homodyne detectors.

similar configuration depicted in Fig. 1 (b), it is expected that the quantum filter (i.e., the best continuous-time estimator) brings us more information, and as consequence we will have chance to construct a better controller than in the standard case without entanglement. The idea of entanglement-assisted feedback control is briefly mentioned in [19], but there has been no quantitative analysis of this control strategy. That is, we are interested in the following questions; (i) *How much does the entanglement-assisted strategy improve the control performance in a realistic setup?* (ii) *In what situation is the entanglement-assisted feedback control really beneficial?* Note that the answers to these questions are non-trivial, because, for a realistic noisy system, the entanglement-assisted feedback control will not always outperform the standard one without entanglement, due to the fragile nature of entangled states.

In this paper, we consider the setup illustrated in Fig. 2. The system to be controlled is a general linear quantum system such as an optical amplifier and an opto-mechanical oscillator [20, 21, 22, 23, 24, 25]. The probe input is given by an optical entangled state generated by combining a squeezed field and a coherent field [26] at a beam splitter; one portion of this entangled field couples to the system while the other portion does not, as in the scheme shown in Fig. 1 (b), and then the combined output field is continuously measured by Homodyne detectors. Finally, based on the measurement signal, we construct the quantum filter and then apply a feedback control to the system. The point of this setting is that the system state is always Gaussian, and as a result the quantum filter is simplified to the *quantum Kalman filter* [27], which enables us to compute the exact real-time estimate of the system variables. Furthermore, in this paper, we consider the quantum *Linear Quadratic Gaussian (LQG)* optimal control problem, meaning that the control goal is to minimize a quadratic-type cost function. Fortunately, again thanks to the Gaussianity of the system state, this problem can be analytically solved by almost the same way as in the classical case [28, 29]. An important fact in this formulation is that a strict lower bound of the cost, which is ideally achievable by employing the so-called *cheap control* [30, 31, 32], is represented by a function of only the estimation error. Therefore this ultimate limit of the LQG control cost has the meaning of SQL, when the input is given by a coherent or a vacuum field.

In the above described framework, first, this paper proves that, thanks to the entangled probe input, the filter certainly gains additional information which may improve the control performance. Next we

study a feedback cooling problem of an opto-mechanical oscillator [33, 34, 35, 36, 37, 38] and provide answers to the above-posed questions by conducting detailed numerical simulations. In particular, it is shown that, by carefully choosing the system parameters ($\theta, \beta_1, \beta_2, \phi_1, \phi_2$; see Fig. 2), the entanglement-assisted feedback control can lower the stationary occupation number of the oscillator below the SQL in the sense of cheap control mentioned above, and moreover, it outperforms the control with an optimized squeezed probe field [13].

Finally, we note that the scheme presented in this paper differs from that studied in [36], which considers the use of system's *internal* entanglement to enhance cooling for an opto-mechanical system.

Notation: \Re and \Im denote the real and imaginary parts, respectively. I_n : $n \times n$ identity matrix. O_n : $n \times n$ zero matrix. $0_{n \times m}$: $n \times m$ zero matrix.

2 Quantum Kalman filtering, LQG control, and cheap control

We here review the general theory of quantum Kalman filtering, LQG optimal control, and the cheap control.

2.1 Quantum linear systems

In this paper we consider a linear quantum system, whose general form is described as follows (see [15, 16, 21, 24] for more details). The system variables are collected in a vector of operators $\hat{x} := [\hat{q}_1, \hat{p}_1, \dots, \hat{q}_n, \hat{p}_n]^\top$, where \hat{q}_i and \hat{p}_i are position and momentum operators. They satisfy the canonical commutation relation $\hat{q}_i \hat{p}_j - \hat{p}_j \hat{q}_i = i\delta_{ij}$ (we set $\hbar = 1$), which are summarized as

$$\hat{x} \hat{x}^\top - (\hat{x} \hat{x}^\top)^\top = i\Sigma_n, \quad (1)$$

where Σ_n is the following $2n \times 2n$ block diagonal matrix:

$$\Sigma_n = \text{diag}\{\sigma, \dots, \sigma\}, \quad \sigma = \begin{bmatrix} 0 & 1 \\ -1 & 0 \end{bmatrix}.$$

The system variables are governed by the linear dynamics

$$d\hat{x}_t = A\hat{x}_t dt + F u_t dt + B d\hat{W}_t. \quad (2)$$

Note that, in order to preserve Eq. (1) for all t , the matrix A must be of the following form:

$$A = \Sigma_n(G + \Sigma_n^\top B \Sigma_m B^\top \Sigma_n / 2), \quad (3)$$

where G is a $2n \times 2n$ real symmetric matrix determining the system Hamiltonian by $\hat{H} = \hat{x}^\top G \hat{x} / 2$. Also B is a $2n \times 2m$ real matrix determined from the system-field coupling. F is a real matrix and u_t is the vector of classical (i.e., non-quantum) signal representing the control input. The system couples with m probe or environment bosonic fields, with vector of noise operators $\hat{W}_t := [\hat{Q}_1, \hat{P}_1, \dots, \hat{Q}_m, \hat{P}_m]^\top$. This satisfies the quantum Ito rule $d\hat{W}_t d\hat{W}_t^\top = \Theta dt$, with zero mean: $\langle d\hat{W}_t \rangle = 0$. The correlation matrix Θ is $2m \times 2m$ block diagonal Hermitian, and their j th block matrix (i.e., the correlation matrix of \hat{Q}_j and \hat{P}_j) is in general written as

$$\Theta_j = \begin{bmatrix} N_j + \Re(M_j) + 1/2 & \Im(M_j) + i/2 \\ \Im(M_j) - i/2 & N_j - \Re(M_j) + 1/2 \end{bmatrix}. \quad (4)$$

The parameters $N_j \in \mathbb{R}$ and $M_j \in \mathbb{C}$ satisfy $N_j(N_j + 1) \geq |M_j|^2$. Note that N_j represents the average excitation number of the probe quanta, and M_j is related to squeezing of the field; if $N_j(N_j + 1) = |M_j|^2$ is satisfied, the probe field state is a pure squeezed state¹, while if $M_j = 0$ it is not squeezed. Also note that $d\hat{Q}_j d\hat{P}_j - d\hat{P}_j d\hat{Q}_j = idt$.

¹ The field annihilation operator $\hat{A}_1 = (\hat{Q}_1 + i\hat{P}_1)/\sqrt{2}$ for a pure squeeze state is modeled by the Bogoliubov transformation $\hat{A}_1 = \hat{A}_1^{(0)} \cosh(r/2) - \hat{A}_1^{(0)\dagger} e^{i\theta/2} \sinh(r/2)$, where $\hat{A}_1^{(0)}$ is the vacuum field operator. The corresponding parameters N_1 and M_1 are obtained from the definition $d\hat{A}_1 d\hat{A}_1^\dagger = (N_1 + 1)dt$, $d\hat{A}_1^\dagger d\hat{A}_1 = N_1 dt$, $dA_1^2 = M_1 dt$, and $dA_1^{\dagger 2} = M_1^* dt$, which lead to $N_1 = \sinh^2(r/2)$ and $M_1 = -e^{i\theta/2} \sinh(r/2) \cosh(r/2)$. Hence certainly $N_1(N_1 + 1) = |M_1|^2$ is satisfied.

For this system we perform a (joint) Homodyne measurement on ℓ ($\leq m$) output probe fields, which generates the classical measurement signal

$$dy_t = C\hat{x}_t dt + Dd\hat{W}_t. \quad (5)$$

Note that, due to the unitarity of the system-field coupling, the $\ell \times 2n$ real matrix C and the $\ell \times 2m$ real matrix D satisfy the following specific structure:

$$C = D\Sigma_m B^\top \Sigma_n, \quad D\Sigma_m D^\top = 0. \quad (6)$$

In this paper we assume that A is *Hurwitz*, meaning that the real parts of all the eigenvalues of A are negative; hence in this case the mean of the system variables, $\langle \hat{x}_t \rangle$, which obeys the dynamics $d\langle \hat{x}_t \rangle / dt = A\langle \hat{x}_t \rangle$, converges to zero in the long time limit, i.e., $\langle \hat{x}_t \rangle \rightarrow 0$. Note that the opto-mechanical system studied in Section 4 is Hurwitz.

2.2 Quantum Kalman filter

Let us consider the situation where we want to perform a real-time estimate of the system variable \hat{x}_t based on the measurement signal y_t . The solution is provided by the quantum filtering theory; that is, we can rigorously define the quantum conditional expectation $\pi(\hat{x}_t) := \mathbb{E}(\hat{x}_t | \mathcal{Y}_t)$, where \mathcal{Y}_t is the σ -algebra composed of the measurement signal $\{y_s | 0 \leq s \leq t\}$. In fact the classical random variable $\pi(\hat{x}_t)$ is the least mean squared estimate of \hat{x}_t . The recursive equation updating $\pi(\hat{x}_t)$ is given by the quantum Kalman filter [27, 28, 29]:

$$\begin{aligned} d\pi(\hat{x}_t) &= A\pi(\hat{x}_t)dt + Fu_t dt + K_t(dy_t - C\pi(\hat{x}_t)dt), \\ K_t &= (V_t C^\top + B\Re(\Theta)D^\top)(D\Re(\Theta)D^\top)^{-1}, \end{aligned} \quad (7)$$

where the initial condition is $\pi(\hat{x}_0) = \langle \hat{x}_0 \rangle$ with $\langle \bullet \rangle$ the unconditional expectation. V_t is the estimation error covariance matrix defined as

$$V_t := \langle \Delta\hat{x}_t \Delta\hat{x}_t^\top + (\Delta\hat{x}_t \Delta\hat{x}_t^\top)^\top \rangle / 2, \quad \Delta\hat{x}_t := \hat{x}_t - \pi(\hat{x}_t),$$

which evolves in time according to the following Riccati differential equation:

$$\dot{V}_t = AV_t + V_t A^\top + B\Re(\Theta)B^\top - K_t D\Re(\Theta)D^\top K_t^\top. \quad (8)$$

Under the assumption A being Hurwitz², this equation has a unique steady solution $V_\infty > 0$.

2.3 Quantum LQG control

In the infinite horizon quantum LQG control problem, we consider the following cost function:

$$J[u] = \lim_{T \rightarrow \infty} \frac{1}{T} \left\langle \int_0^T (\hat{x}_t^\top Q \hat{x}_t + u_t^\top R u_t) dt \right\rangle, \quad (9)$$

where $Q \geq 0$ and $R > 0$ are real weighting matrices. The goal is to design the feedback control law u_t as a function of y_t , that minimizes the cost (9) under the condition (2), i.e., $u_t^* = \arg \min_u J[u]$. The point is that, due to the tower property $\langle \hat{x}_t \rangle = \langle \pi(\hat{x}_t) \rangle = \langle \mathbb{E}(\hat{x}_t | \mathcal{Y}_t) \rangle$, the cost can be represented in terms of only the filter variable as follows. That is, due to the relation $\mathbb{E}(\hat{x}_t \hat{x}_t^\top | \mathcal{Y}_t) = V_t + i\Sigma_n/2 + \pi(\hat{x}_t)\pi(\hat{x}_t)^\top$, we have

$$\begin{aligned} \left\langle \int_0^T (\hat{x}_t^\top Q \hat{x}_t + u_t^\top R u_t) dt \right\rangle &= \left\langle \int_0^T \left(\text{Tr} [Q \mathbb{E}(\hat{x}_t \hat{x}_t^\top | \mathcal{Y}_t)] + u_t^\top R u_t \right) dt \right\rangle \\ &= \left\langle \int_0^T \left(\pi(\hat{x}_t)^\top Q \pi(\hat{x}_t) + u_t^\top R u_t \right) dt \right\rangle + \int_0^T \text{Tr} \left[Q \left(V_t + \frac{i}{2} \Sigma_n \right) \right] dt, \end{aligned}$$

² Note that the Hurwitz property is a sufficient condition for Eq. (8) to have a unique steady solution. A useful necessary and sufficient condition is that (A^\top, D) is stabilizable and (A^\top, B) is detectable [39].

where we have used the fact that V_t obeys the deterministic time evolution (8). Hence this equation leads to

$$J[u] = \lim_{T \rightarrow \infty} \frac{1}{T} \left\langle \int_0^T \left(\pi(\hat{x}_t)^\top Q \pi(\hat{x}_t) + u_t^\top R u_t \right) dt \right\rangle + \text{Tr}(QV_\infty). \quad (10)$$

Note that the second term is constant. As a result, our problem is to find u_t minimizing the first term of Eq. (10) under the condition (7). This is exactly the *classical* LQG control problem and can be analytically solved as follows (see [40] or Appendix A); the optimal control input is given by

$$u_t^* = -R^{-1} F^\top P_t \pi(\hat{x}_t), \quad (11)$$

where P_t is the solution of the following Riccati equation:

$$\dot{P}_t + P_t A + A^\top P_t - P_t F R^{-1} F^\top P_t + Q = 0. \quad (12)$$

Likewise the case of Eq. (8), because A is Hurwitz³, this equation has a unique steady solution $P_\infty \geq 0$. The minimum value of the cost, which is reached by the optimal control (11), is given by

$$J[u^*] = \text{Tr}(K_\infty D \Re(\Theta) D^\top K_\infty^\top P_\infty) + \text{Tr}(QV_\infty). \quad (13)$$

Note that u_t^* is a function of the optimal estimate $\pi(\hat{x}_t)$. Thus, we can design the optimal estimate and control separately; this is called the *separation principle* as in the classical case [41].

2.4 Lower bound of the minimum cost: The cheap control

Let us set $R = \epsilon^2 I$ for the cost function (9), where $\epsilon > 0$ is a positive scalar, and use P_ϵ to denote the solution of the Riccati equation (12). Then, it was proven in [30] that P_ϵ monotonically decreases as ϵ goes to zero. Moreover, we have that $\lim_{\epsilon \rightarrow 0} P_\epsilon = 0$, if and only if the system characterized by (A, F, \bar{Q}) is *minimum phase* and *right invertible*; see Appendix B for the definitions of this condition (\bar{Q} is a real matrix satisfying $Q = \bar{Q}^\top \bar{Q}$). In this case, the steady solution of the Riccati equation (12) takes the form $P_\infty = \epsilon \bar{P} + O(\epsilon^2)$. Then, the minimum cost (13) becomes

$$J[u^*] = \epsilon \text{Tr}(K_\infty D \Re(\Theta) D^\top K_\infty^\top \bar{P}) + \text{Tr}(QV_\infty) + O(\epsilon^2), \quad (14)$$

and the optimal control input (11) is given by $u_t^* = -\epsilon^{-1} F^\top \bar{P} \pi(\hat{x}_t)$ at steady state. Now we consider the situation where the actuator is allowed to have a large control gain (e.g., the case $\epsilon \approx 0$); in particular, the control input in the ideal limit $\epsilon \rightarrow +0$, meaning that no penalty is imposed on it, is called the cheap control [30, 31, 32]. We then see that this ultimate feedback control perfectly suppresses the fluctuation of the estimated variables $\pi(\hat{x}_t)$, i.e., the first term of Eq. (14), and as a result the total cost is limited only by the optimal estimation error. Therefore, we can take $J^*[u^*] = \text{Tr}(QV_\infty)$ as a fundamental quantity that is reasonably used for evaluating the performance of feedback control, because it cannot be further decreased by any control. In particular, we define the SQL as the value of $J^*[u^*]$ when the probe input is given by a coherent or a vacuum field. Finally note that, when $\epsilon \rightarrow +0$, Eq. (9) equals to the stationary energy $\langle \hat{x}_\infty^\top Q \hat{x}_\infty \rangle$, and this can be ultimately reduced, by the ideal cheap control, to $J^*[u^*] = \text{Tr}(QV_\infty)$.

3 Configuration of the entanglement-assisted feedback control

3.1 Model

The entanglement-assisted feedback control configuration considered in this paper is depicted in Fig. 2. This model has the following four features.

- (i) The system is linear and couples with a single probe field.

³ As mentioned in the footnote 2, this condition is stronger than the condition (A, F) being stabilizable and (A, \sqrt{Q}) begin detectable, which is a necessary and sufficient condition for Eq. (12) to have a unique steady solution $P_\infty \geq 0$. Note that, in this case, $A - FR^{-1}F^\top P_\infty$ is Hurwitz, meaning that the controlled filter equation is stable.

(ii) The entangled optical field is produced by combining a fixed squeezed field \hat{W}_1 and a fixed coherent field \hat{W}_2 , at a beam splitter (BS1). The correlation matrices (4) of these fields are respectively given by

$$\Theta_1 = \frac{1}{2} \begin{bmatrix} \cos \theta & -\sin \theta \\ \sin \theta & \cos \theta \end{bmatrix} \begin{bmatrix} e^{-r} & i \\ -i & e^r \end{bmatrix} \begin{bmatrix} \cos \theta & \sin \theta \\ -\sin \theta & \cos \theta \end{bmatrix}, \quad \Theta_2 = \frac{1}{2} \begin{bmatrix} 1 & i \\ -i & 1 \end{bmatrix},$$

where r is the squeezing level and θ represents the phase of the squeezed state in the phase space; see Fig. 2 and the footnote in page 5. The reflectivity of BS1 is, for simplicity, set to β_1^2 with $0 \leq \beta_1 \leq 1$. Note that, for all $\beta_1 \in (0, 1)$, the output fields of BS1 are entangled (see Appendix C). As shown in the figure, one portion of this entangled field couples with the system, while the other portion does not. The degree of entanglement can be changed by tuning β_1 , while maintaining the total amount of energy for producing this entangled field. Hence we can conduct a fair comparison of the entanglement-assisted control method (the case $0 < \beta_1 < 1$) and the standard method without entanglement (the case $\beta_1 = 0, 1$), given the same amount of resources. In particular, note that the SQL corresponds to the case $\beta_1 = 1$.

(iii) We assume that the system's output field is subjected to an optical loss, which can be modeled by introducing a fictitious beam splitter with reflectivity δ^2 ; if $\delta = 0$, then there is no optical loss. \hat{W}_3 denotes the vacuum noise field coming into this fictitious beam splitter, whose correlation matrix is the same as that of \hat{W}_2 , i.e., $\Theta_3 = \Theta_2$. As consequence the overall system contains three input fields \hat{W}_1 , \hat{W}_2 , and \hat{W}_3 , implying that $m = 3$ in the system equations (2) and (5). The total correlation matrix is thus given by

$$\Theta = \text{diag}\{\Theta_1, \Theta_2, \Theta_3\}.$$

Note again that \hat{W}_1 and \hat{W}_2 represent the probe fields, while \hat{W}_3 denotes the unwanted noise field.

(iv) The system's output field after being subjected to the optical loss meets the other portion of the entangled input field, at the second beam splitter (BS2) with reflectivity β_2^2 ; again for simplicity we assume $0 \leq \beta_2 \leq 1$. Then the final output fields are measured by two Homodyne detectors with phase ϕ_1 and ϕ_2 , which generate two output signals y_1 and y_2 . Note that, if $\beta_2 = 0$ or $\beta_2 = 1$, the two optical fields are not combined at BS2 and are measured independently; this type of measurement is called the local measurement. The other case with $0 < \beta_2 < 1$ is called the global measurement.

The overall system dynamics realizing the above setup is given as follows. First we use the fact that, for a general open linear system interacting with a single probe field, the system-field coupling is represented by an operator (the so-called Lindblad operator) of the form $\hat{L} = c^\top \hat{x}$ with c the $2n$ -dimensional complex column vector, and this determines the B matrix in Eq. (2) as follows (see e.g., [15, 16, 24]). That is, by defining the $2 \times 2n$ real matrix

$$\bar{C} = \sqrt{2} \begin{bmatrix} \Re(c)^\top \\ \Im(c)^\top \end{bmatrix}, \quad (15)$$

we can specify the B matrix in the following form:

$$B = [\alpha_1 \Sigma_n \bar{C}^\top \Sigma_1, \beta_1 \Sigma_n \bar{C}^\top \Sigma_1, 0_{2n \times 2}], \quad (16)$$

where $\alpha_1 = \sqrt{1 - \beta_1^2}$. Then the A matrix is determined by Eq. (3) with G specified by the system Hamiltonian $\hat{H} = \hat{x}^\top G \hat{x} / 2$. The C matrix is also specified by Eq. (6) and is now given by

$$C = D \Sigma_3 B^\top \Sigma_n = D \begin{bmatrix} \alpha_1 \bar{C} \\ \beta_1 \bar{C} \\ 0_{2 \times 2n} \end{bmatrix}. \quad (17)$$

Here D is a 2×6 real matrix of the form

$$D = [D_1, D_2, O_2] T_2 T_L T_1,$$

where

$$D_1 = \begin{bmatrix} \cos \phi_1 & \sin \phi_1 \\ 0 & 0 \end{bmatrix}, \quad D_2 = \begin{bmatrix} 0 & 0 \\ \cos \phi_2 & \sin \phi_2 \end{bmatrix}$$

and

$$T_k = \begin{bmatrix} \alpha_k I_2 & \beta_k I_2 & O_2 \\ -\beta_k I_2 & \alpha_k I_2 & O_2 \\ O_2 & O_2 & I_2 \end{bmatrix} \quad (k = 1, 2), \quad T_L = \begin{bmatrix} \sqrt{1 - \delta^2} I_2 & O_2 & \delta I_2 \\ O_2 & I_2 & O_2 \\ -\delta I_2 & O_2 & \sqrt{1 - \delta^2} I_2 \end{bmatrix},$$

with $\alpha_2 = \sqrt{1 - \beta_2^2}$. Note that T_1 and T_2 represent the scattering process at BS1 and BS2, respectively. Also T_L corresponds to the optical loss in the system's output field. D_1 and D_2 represent the Homodyne measurements with phase ϕ_1 and ϕ_2 , respectively.

3.2 Information gain via entanglement

This subsection is devoted to show that, in a special setup, an additional information about the system is indeed obtained through the second path in the interferometer, which may improve the control performance. That is, we consider the case where the system's output field completely diminishes, i.e., $\delta = 1$. In this case, the D matrix is given by

$$D = [-\beta_1(\beta_2 D_1 + \alpha_2 D_2), \alpha_1(\beta_2 D_1 + \alpha_2 D_2), \alpha_2 D_1 - \beta_2 D_2],$$

and as a result $C = 0$ for any choice of \bar{C} . Then the system equations (2) and (5) are given by

$$d\hat{x}_t = A\hat{x}_t dt + Fu_t dt + Bd\hat{W}_t, \quad dy_t = Dd\hat{W}_t. \quad (18)$$

Hence, as expected, the measurement output y_t does not *explicitly* contain any information about the system. However, interestingly, the observer can *implicitly* gain information; intuitively, this is because the observer knows that the *same* noise \hat{W}_t enters into the system and the detector; in other words, the observer exactly knows the noise that drives the system and thus can track the estimate of the system's time-evolution. Actually, the quantum Kalman filter equation (7) is now given by

$$d\pi(\hat{x}_t) = A\pi(\hat{x}_t)dt + Fu_t dt + B\Re(\Theta)D^\top (D\Re(\Theta)D^\top)^{-1} dy_t, \quad (19)$$

which means that the observer can update the estimate $\pi(\hat{x}_t)$ using the measurement result y_t . Also the estimation error covariance matrix follows

$$\dot{V}_t = AV_t + V_t A^\top + B\Re(\Theta)B^\top - B\Re(\Theta)D^\top (D\Re(\Theta)D^\top)^{-1} D\Re(\Theta)B^\top. \quad (20)$$

Now, because A is Hurwitz, V_t has a steady solution, meaning that the estimation error is bounded. The above two equations indicate that the important term bringing the information to the filter (19) and (20) is $B\Re(\Theta)D^\top$, which is now calculated as

$$B\Re(\Theta)D^\top = \frac{\alpha_1 \beta_1}{2} \Sigma_n \bar{C}^\top \Sigma_1 [I_2 - 2\Re(\Theta_1)] (\beta_2 D_1^\top + \alpha_2 D_2^\top).$$

If there is no entanglement (i.e., $r = 0$ or $\alpha_1 \beta_1 = 0$), then $B\Re(\Theta)D^\top = 0$, and the filter equations are reduced to

$$d\pi(\hat{x}_t) = A\pi(\hat{x}_t)dt + Fu_t dt, \quad \dot{V}_t = AV_t + V_t A^\top + B\Re(\Theta)B^\top.$$

These are simply the dynamics of unconditional expectation $\pi(\hat{x}_t) = \langle \hat{x}_t \rangle$ and the error covariance matrix, which correspond to the master equation describing the statistical time-evolution of the system without measurement. Therefore it is now clear that the entanglement-assisted filter gains additional information about the system through the entangled input field. However, note that an additional information does not always improve the control performance, because, as demonstrated in Section 4.5, an entangled probe field is generally fragile and as a result the system's output field becomes more noisy compared to the case of coherent input.

Remark: The measurement output $dy_t = Dd\hat{W}_t$ in Eq. (18) has the form of *no-knowledge measurement* [42], which can be used to cancel decoherence. Interestingly, unlike the measurement scheme presented here, the no-knowledge one does not provide any information to the observer; actually for the setup of [42] it can be proven that A is not Hurwitz and the estimation error diverges.

4 Entanglement-assisted feedback for opto-mechanical oscillator

In this section, we conduct detailed numerical simulations to evaluate how much the proposed entanglement-assisted feedback control scheme is effective in a practical setup.

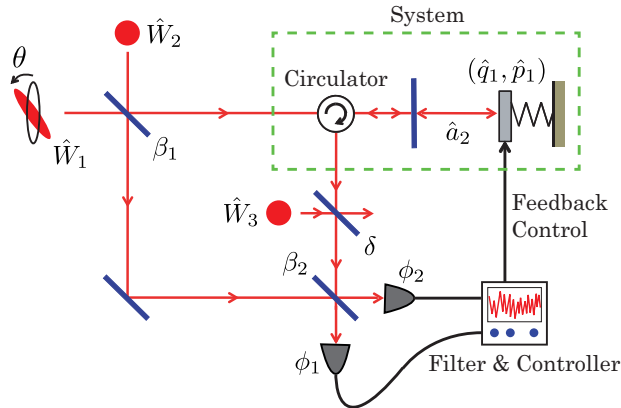


Figure 3: Opto-mechanical oscillator coupled to the entangled probe field.

4.1 System model

The system of interest is an opto-mechanical oscillator shown in Fig. 3. Let (\hat{q}_1, \hat{p}_1) be the position and momentum operators of the mechanical oscillator, and \hat{a}_2 be the annihilation operator of the optical cavity. The system Hamiltonian is given by

$$\hat{H} = \frac{\omega}{2}(\hat{q}_1^2 + \hat{p}_1^2) + \frac{\Delta}{2}(\hat{q}_2^2 + \hat{p}_2^2) - \lambda\hat{q}_1\hat{q}_2, \quad (21)$$

where ω is the resonant frequency of the oscillator and Δ is the frequency detuning of the cavity mode in the rotating frame of the driving laser frequency; see [33, 36, 43] for more detailed description. Note $\hat{q}_2 = (\hat{a}_2 + \hat{a}_2^\dagger)/\sqrt{2}$ and $\hat{p}_2 = (\hat{a}_2 - \hat{a}_2^\dagger)/\sqrt{2}i$. The third term is the linearized radiation pressure force with strength $|\lambda|$, representing the interaction between the oscillator and the cavity field. From the relation $\hat{H} = \hat{x}^\top G \hat{x}/2$ with $\hat{x} = [\hat{q}_1, \hat{p}_1, \hat{q}_2, \hat{p}_2]^\top$, we have

$$G = \left[\begin{array}{cc|cc} \omega & 0 & -\lambda & 0 \\ 0 & \omega & 0 & 0 \\ \hline -\lambda & 0 & \Delta & 0 \\ 0 & 0 & 0 & \Delta \end{array} \right].$$

The system couples to the driving laser field at the partially reflective end-mirror of the cavity, with strength κ ; this coupling is represented by the following operator:

$$\hat{L} = \sqrt{\kappa}\hat{a}_2 = \sqrt{\frac{\kappa}{2}}(\hat{q}_2 + i\hat{p}_2) = \sqrt{\frac{\kappa}{2}}[0, 0, 1, i]\hat{x}.$$

Thus, Eq. (15) yields

$$\bar{C} = \sqrt{\kappa} \left[\begin{array}{cc|cc} 0 & 0 & 1 & 0 \\ 0 & 0 & 0 & 1 \end{array} \right].$$

This determines the system's B and C matrices from Eqs. (16) and (17), respectively, and the A matrix from Eq. (3). In addition, we assume that the oscillator is subjected to a thermal environment with mean photon number \bar{n}_{th} . Then the system matrices are modified as follows; we need to change the A matrix to $A - \gamma\Gamma/2$ and the constant term in the Riccati equation (8), $B\Re(\Theta)B^\top$, to $B\Re(\Theta)B^\top + \gamma(\bar{n}_{\text{th}} + 1/2)\Gamma$, where γ represents the system-environment coupling strength and $\Gamma = \text{diag}\{1, 1, 0, 0\}$. Note that $A - \gamma\Gamma/2$ is Hurwitz, meaning that both the Riccati equations (8) and (12) have a unique steady solution. The oscillator can be directly controlled by implementing a piezo-actuator [44] (the case shown in Fig. 3) or indirectly controlled by modulating the input probe field. In both cases, it can be shown that the system satisfies the conditions for the cheap control described in Section 2.4; see Appendix B.

4.2 Control goal

The control goal is to cool the oscillator toward its motional ground state; i.e., we want to minimize the stationary mechanical occupation number

$$\bar{n} = \langle \hat{a}_{1,\infty}^\dagger \hat{a}_{1,\infty} \rangle = (\langle \hat{q}_{1,\infty}^2 \rangle + \langle \hat{p}_{1,\infty}^2 \rangle - 1)/2.$$

As described in Section 2.4, this can be ultimately reduced, by the ideal cheap control, to

$$\bar{n}^* = (\text{Tr}(\Gamma V_\infty) - 1)/2, \quad (22)$$

where again $\Gamma = \text{diag}\{1, 1, 0, 0\}$ and V_∞ is the steady solution of the Riccati equation (8).

The system parameters are set to the following typical values (in the unit $\omega = 1$) in the feedback cooling setup (e.g., [36]). First we assume the resonant driving $\Delta = 0$, meaning that the oscillator's position and momentum can be best estimated by the filter and accordingly controlled efficiently. Also the cavity line width is set to $\kappa = 2$ (bad cavity regime), so that the intra cavity field immediately leaks to outside and as a consequence the oscillator dynamics can be well observed by the filter. The oscillator is subjected to a thermal noise with mean photon number $\bar{n}_{\text{th}} = 1 \times 10^5$ with coupling strength $\gamma = 1 \times 10^{-7}$. The squeezing level of the probe field is set to $r = 2.3$ (10 dB squeezing), which is accessible with the current technology.

In this setting, the task is to optimize the parameters $(\beta_1, \beta_2, \phi_1, \phi_2, \theta)$ so that Eq. (22) is minimized. To see how to find those optimal parameters, let us assume the lossless setup (i.e., $\delta = 0$) and focus on only the oscillator mode, where the cavity mode is adiabatically eliminated. This dynamical equation is obtained by setting $d\hat{q}_2 = 0$ and $d\hat{p}_2 = 0$ due to $\kappa \gg \gamma$ and eventually eliminating (\hat{q}_2, \hat{p}_2) from the whole dynamical equation;

$$d\hat{q}_1 = -\frac{\gamma}{2}\hat{q}_1 dt + \omega\hat{p}_1 dt - \sqrt{\gamma}d\hat{Q}_{\text{th}}, \quad (23)$$

$$d\hat{p}_1 = -\omega\hat{q}_1 dt - \frac{\gamma}{2}\hat{p}_1 dt + u dt - \frac{2\lambda}{\sqrt{\kappa}}(\alpha_1 d\hat{Q}_1 + \beta_1 d\hat{Q}_2) - \sqrt{\gamma}d\hat{P}_{\text{th}}, \quad (24)$$

$$dy_1 = \frac{2\alpha_2\lambda\sin\phi_1}{\sqrt{\kappa}}\hat{q}_1 dt - (\alpha_1\alpha_2 + \beta_1\beta_2)(\cos\phi_1 d\hat{Q}_1 + \sin\phi_1 d\hat{P}_1) \\ + (\alpha_1\beta_2 - \beta_1\alpha_2)(\cos\phi_1 d\hat{Q}_2 + \sin\phi_1 d\hat{P}_2), \quad (25)$$

$$dy_2 = -\frac{2\beta_2\lambda\sin\phi_2}{\sqrt{\kappa}}\hat{q}_1 dt + (\alpha_1\beta_2 - \beta_1\alpha_2)(\cos\phi_2 d\hat{Q}_1 + \sin\phi_2 d\hat{P}_1) \\ + (\alpha_1\alpha_2 + \beta_1\beta_2)(\cos\phi_2 d\hat{Q}_2 + \sin\phi_2 d\hat{P}_2), \quad (26)$$

where u represents the magnitude of the force applied to a piezo-actuator mounted on the oscillator, and $(\hat{Q}_{\text{th}}, \hat{P}_{\text{th}})$ are the quadrature of the thermal field. These equations lead to a rough guide for choosing the parameters, as follows.

1. First, the bigger the first terms in Eqs. (25) and (26) become, the more information the observer gains. Hence, it would be reasonable to make the terms $\sin\phi_1$ and $\sin\phi_2$ bigger, or equivalently take $\phi_1 \approx \pi/2$ and $\phi_2 \approx \pi/2$.
2. The above choice of (ϕ_1, ϕ_2) implies that the measurement outputs are dominantly affected by the phase-quadrature noise (\hat{P}_1, \hat{P}_2) rather than the amplitude quadrature noise (\hat{Q}_1, \hat{Q}_2) . Then by squeezing \hat{P}_1 , we can improve the signal to noise ratio both in y_1 and y_2 . This means that $\theta \approx \pi/2$ would be a proper choice.
3. The coefficients of the noise terms related to $\hat{W}_1 = [\hat{Q}_1, \hat{P}_1]^\top$ and $\hat{W}_2 = [\hat{Q}_2, \hat{P}_2]^\top$ in y_1 and y_2 cannot be simultaneously reduced, because they satisfy $(\alpha_1\alpha_2 + \beta_1\beta_2)^2 + (\alpha_1\beta_2 - \beta_1\alpha_2)^2 = 1$. Then, because \hat{W}_2 is not a tunable noise field, meaning that $\langle (\cos\phi_1 d\hat{Q}_2 + \sin\phi_1 d\hat{P}_2)^2 \rangle = dt$ and $\langle (\cos\phi_2 d\hat{Q}_2 + \sin\phi_2 d\hat{P}_2)^2 \rangle = dt$, it would be reasonable to choose the BS parameters so that the coefficient of \hat{W}_2 is reduced; more precisely, $\alpha_1\beta_2 - \beta_1\alpha_2 \approx 0$ if y_1 is mainly used (i.e., $\alpha_2 \approx 1$), or $\alpha_1\alpha_2 + \beta_1\beta_2 \approx 0$ if y_2 is mainly used (i.e., $\beta_2 \approx 1$). This leads to $(\alpha_1, \beta_1, \alpha_2, \beta_2) \approx (1, 0, 1, 0)$ or $(\alpha_1, \beta_1, \alpha_2, \beta_2) \approx (1, 0, 0, 1)$.

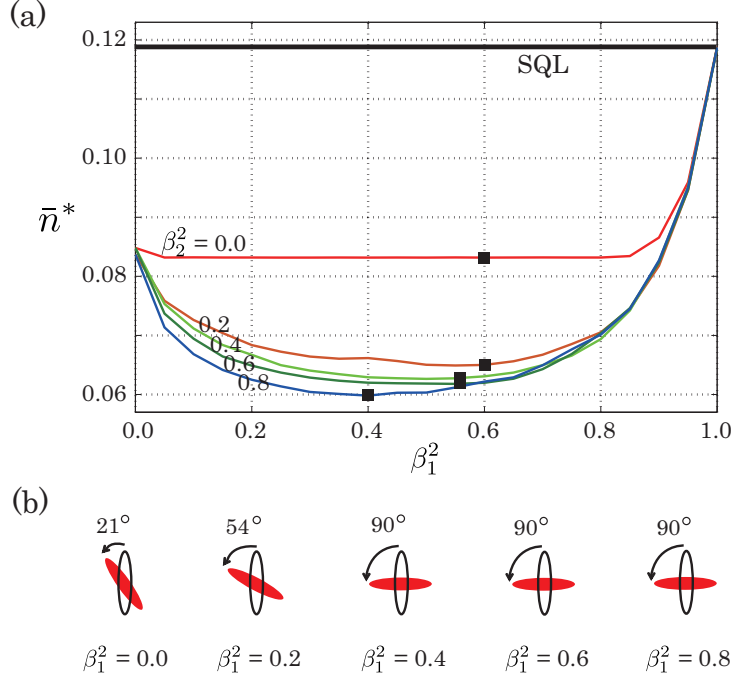


Figure 4: (a) The achievable lowest mechanical occupation number, \bar{n}^* , versus β_1^2 (the reflectivity of BS1) for several values of β_2^2 , for the case $\lambda = 0.3$ and $\delta = 0$. At each point of β_1 , the phase of the squeezed field and the Homodyne detection, (θ, ϕ_1, ϕ_2) , are optimized. The black box indicates the minimum of \bar{n}^* . (b) The optimal phase θ of the squeezed field at each β_1 for the case $\beta_2^2 = 0.8$.

Of course, the above intuitive observation, particularly the last one, would not be necessarily true. In fact, we have now arrived at $(\alpha_1, \beta_1) \approx (1, 0)$, but this means that the input probe field is nearly a separable state where the squeezed component is injected to the system, and the entanglement property is not effectively used. Moreover, when $(\alpha_1, \beta_1) \approx (1, 0)$, the back-action noise on \hat{p}_1 (i.e., the fourth term in the right-hand side of Eq. (24)) is dominated by $d\hat{Q}_1$; however, because now \hat{Q}_1 is nearly *anti-squeezed* (due to $\theta \approx \pi/2$), this parameter choice induces a bigger back-action noise. Therefore, the parameters have to be carefully chosen, via detailed numerical simulations taking into account the tradeoff between the back-action noise and the signal to noise ratio for the measurement outputs y_1 and y_2 .

4.3 Effectiveness of the entanglement-assisted feedback control

First let us see if the entanglement would actually bring any advantage to the feedback control. Figure 4 (a) shows \bar{n}^* as a function of the reflectivity of BS1, β_1^2 , in the case $\lambda = 0.3$ (weak coupling regime) and $\delta = 0$ (the system's output field has no loss). \bar{n}^* is calculated from Eq. (22) together with the steady solution V_∞ of the Riccati equation (8). Furthermore, it is minimized with respect to the phase of the probe squeezed field, θ , and the phases of the two Homodyne detectors, (ϕ_1, ϕ_2) , at each β_1 ; Figure 4 (b) illustrates the optimal θ at each β_1 for the case $\beta_2^2 = 0.8$. The reflectivity β_1^2 represents how much the squeezed field \hat{W}_1 is split into two arms, which determines the amount of entanglement. Note that when $\beta_1 = 0$ or $\beta_1 = 1$, the input fields are not entangled. In particular, $\beta_1 = 1$ corresponds to the standard case where only the coherent field is injected to the system; hence the value of \bar{n}^* in this case has the meaning of SQL, which is now $\bar{n}_{\text{SQL}}^* \approx 0.119$ as indicated in the figure (a). The five solid curves in the figure (a) show \bar{n}^* for several values of β_2^2 , the reflectivity of BS2; recall that $\beta_2 = 0$ means the case of local measurement, while the cases $\beta_2 \neq 0$ correspond to the global measurement (see (iv) in Section 3.1). Importantly, in all cases the minimum of \bar{n}^* , which is indicated by the black box, is smaller than the SQL and is attained at a certain point of $\beta_1 \in (0, 1)$, where the input field is entangled. In particular, the most effective feedback cooling is carried out when we use the highly entangled probe field with $\beta_1^2 = 0.4$

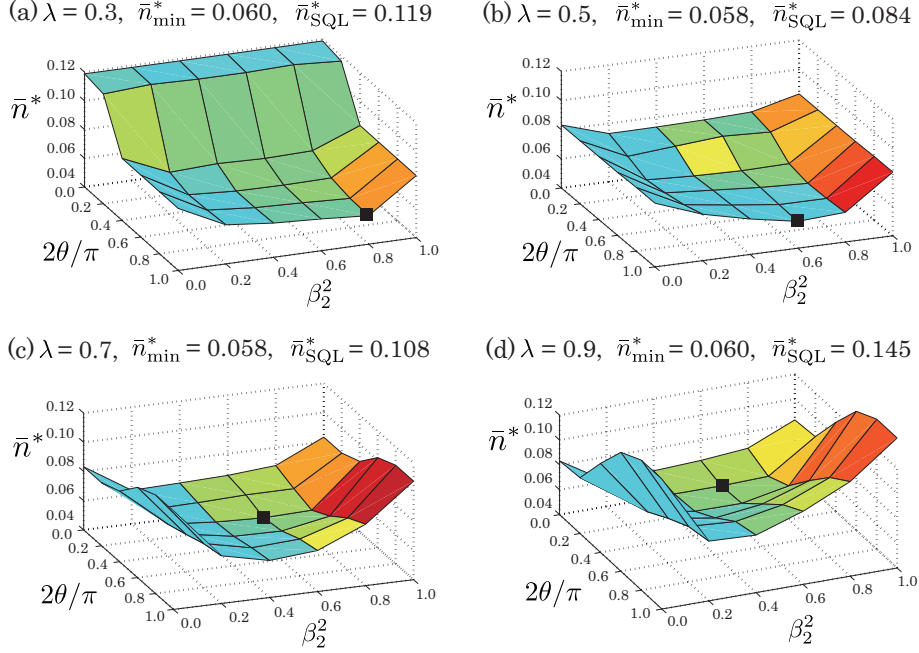


Figure 5: The achievable lowest mechanical occupation number, \bar{n}^* , as a function of θ (phase of the squeezed field) and β_2^2 (reflectivity of BS2), for $\delta = 0$ and several values of λ (strength of the radiation pressure). The black box indicates the minimum of \bar{n}^* .

and perform the global measurement with $\beta_2^2 = 0.8$, in which case the minimum of \bar{n}^* is about 0.06. As a conclusion, the entanglement-assisted feedback control is in fact effective and realizes further cooling of the oscillator below the SQL. The followings are the list of other notable features of this system.

- For the cases $\beta_1^2 = 0.4, 0.6, 0.8$, the optimal phase of the squeezed field is $\theta = \pi/2$. The optimality of $\theta = \pi/2$ was indeed expected in the second observation in Section 4.2 (page 13), but β_1 is not nearly zero, which is not consistent with the third observation in Section 4.2. Therefore, the numerical solver has actually chosen a nontrivial set of parameters that balances the back-action noise on \hat{p}_1 and the measurement noise on (y_1, y_2) .
- The minimum of \bar{n}^* is reached at $\beta_1^2 \neq 0.5$ and $\theta = \pi/2$. This means that the maximal entangled field is not the best probe for the estimation and feedback control; see Appendix C.
- The entanglement-assisted method outperforms the control with the optimized squeezed probe field [13], which corresponds to the case $\beta_1 = 0$.

4.4 Coupling strength and optimal probe

Here we study how much the minimum occupation number \bar{n}_{\min}^* changes with respect to the coupling strength λ . Figure 5 shows \bar{n}^* as a function of θ and β_2 , for $\delta = 0$ and several values of λ . In each figure (a)-(d), \bar{n}^* is already minimized with respect to $(\beta_1, \phi_1, \phi_2)$, and the achieved \bar{n}_{\min}^* is shown together with \bar{n}_{SQL}^* . In particular, in each figure, the optimal value of β_1 has been chosen as: (a) $\beta_1^2 = 0.40$, (b) $\beta_1^2 = 0.65$, (c) $\beta_1^2 = 0.55$, and (d) $\beta_1^2 = 0.50$, implying that the input probe field is highly entangled in all cases. Hence, we end up with the same conclusion that the entanglement-assisted feedback control cools the oscillator below the SQL and even performs better than the case with optimized squeezed probe field.

Note here that, as implied by Eqs. (24), (25), and (26), making λ bigger improves the signal to noise ratio in the measurement output, but at the same time this induces a bigger back-action noise on \hat{p}_1 . Hence, \bar{n}_{SQL}^* does not monotonically change with respect to λ ; interestingly, \bar{n}_{\min}^* takes almost the same value for all λ , which suggests that there would exist a fundamental lower bound of \bar{n}_{\min}^* that

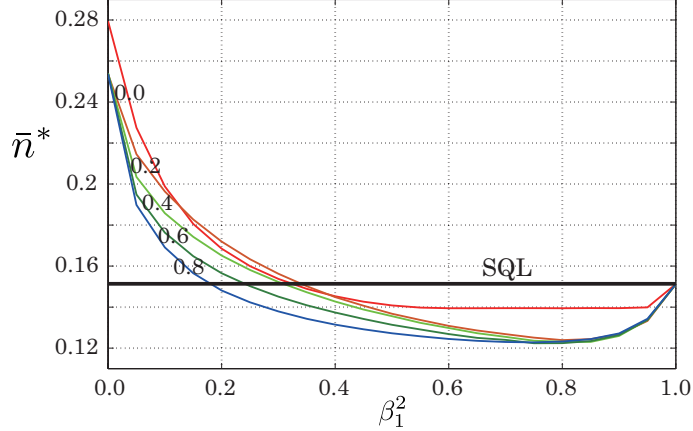


Figure 6: The achievable lowest mechanical occupation number, \bar{n}^* , versus β_1^2 (the reflectivity of BS1) for several values of β_2^2 , for the case $\lambda = 0.3$ and $\delta^2 = 0.1$. At each point of β_1 , the phase of the squeezed light field and the Homodyne detection, (θ, ϕ_1, ϕ_2) , are optimized. The numbers indicated along the curves are the values of β_2^2 , as in the case of Fig. 4.

is independent to λ . Another remarkable fact is that, for small values of λ , the optimal phase of the squeezed field is $\theta = \pi/2$, as seen in the previous subsection; however, this does not hold when λ becomes large. This is because, for a large λ , it is more important to reduce the back-action noise $(2\lambda/\sqrt{\kappa})\alpha_1 d\hat{Q}_1$ than to improve the signal to noise ratio in the measurement process, and thus the squeezed field with $\langle d\hat{Q}_1^2 \rangle < \langle d\hat{P}_1^2 \rangle$ is chosen.

4.5 The case of lossy output field

Next let us consider the case where the system's output field is subjected to the optical loss. Figure 6 is the plot of \bar{n}^* with the same setting as in Fig. 4 (i.e., $\lambda = 0.3$ and (θ, ϕ_1, ϕ_2) are optimized), except that the loss parameter is now set to $\delta^2 = 0.1$. As in the lossless case $\delta = 0$, we find that the minimum of \bar{n}^* is reached when the input probe field is entangled ($\beta_1^2 \approx 0.8$) and the global measurement ($\beta_2^2 = 0.8$) is performed. However, notably, the difference between the minimum value of \bar{n}^* and the SQL given at $\beta_1 = 1$ (i.e., how much the control performance is improved by entanglement) is smaller than the case when $\delta = 0$. That is, the entanglement-assisted feedback is less effective if the system's output field is lossy. Another notable feature is that there is a case where the control performance becomes worse than the SQL via the entanglement-assisted feedback control. This happens when β_1 takes a small value, in which case the portion injected into the system is nearly a pure squeezed field. This result makes sense, because, as is well known, a squeezed field is fragile to noise and the system's output field loses more information than the standard case, which cannot be compensated by the additional information gained from the second path of the interferometer.

Finally Fig. 7 shows the plot of \bar{n}^* as a function of θ and β_2 , for $\lambda = 0.3$ and several values of δ . As in the case of Fig. 5, \bar{n}^* is already minimized with respect to $(\beta_1, \phi_1, \phi_2)$. Note that Fig. 7 (a) is the same as Fig. 5 (a). A notable point is that the optimal values of θ and β_2 in the case $\delta^2 = 0.1$ are the same as those for $\delta = 0$. This means that the optimal input probe field and measurement are independent to the system's output loss δ . This is a desirable fact because an exact value of δ is hard to estimate in practice, but the same input probe field and measurement can be used without respect to δ as long as the system's output loss is enough suppressed. However, Figs. 7 (c) and (d) show that the probe and measurement have to be changed when δ becomes bigger. In this sense, the optimal probe field is not robust for a system with lossy output.

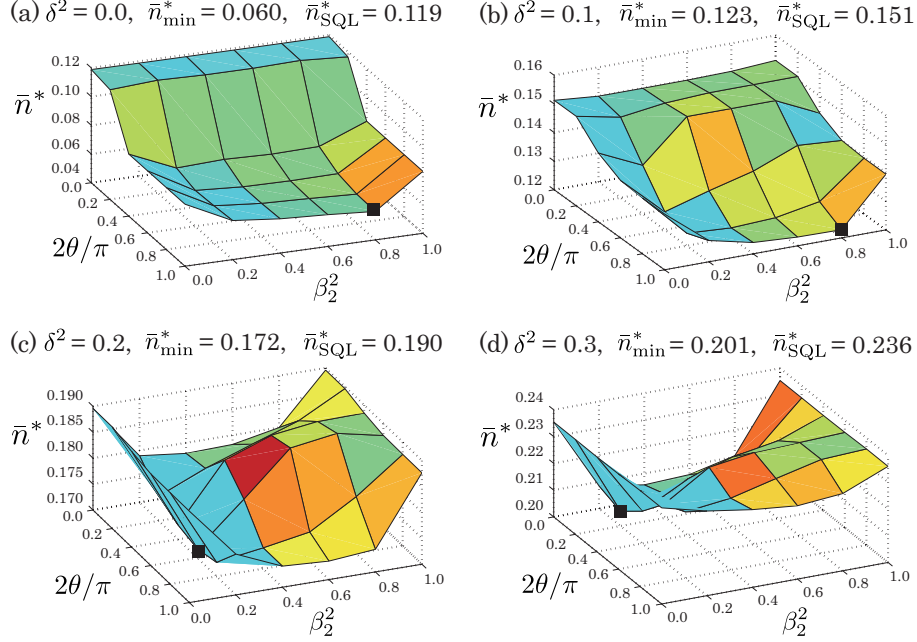


Figure 7: The achievable lowest mechanical occupation number, \bar{n}^* , as a function of θ (phase of the squeezed light field) and β_2^2 (reflectivity of BS2), for $\lambda = 0.3$ and several values of δ (loss in the system's output field). The black box indicates the minimum of \bar{n}^* .

5 Conclusion

In this paper, we have formulated the entanglement-assisted feedback control method for general linear quantum systems, which involves optimization of the amount of entanglement, the phase of the probe squeezed field, and the Homodyne measurement. Thanks to the linear setting, the strict lower bound of LQG cost function, which is achievable by the ideal cheap control, can be explicitly obtained, and it is used to evaluate the control performance. In the detailed numerical simulation studying the cooling problem of an opto-mechanical oscillator, it was shown that the entanglement-assisted controller works better than the standard method without entanglement, i.e., the control with a coherent probe field and even that with an optimized squeezed probe field. Although the improvement is not so drastic especially when the system's output field is lossy, we expect that a significant advantage of the entanglement-assisted method would appear for some nonlinear systems. In fact, it was shown in [45] that, in a different measurement configuration, an entangled probe field can be used to significantly improve the detection efficiency for a qubit system; an extension of this study to the feedback control problem is an interesting future work.

Appendix A: Solution of LQG control problem

Here we briefly explain how to derive the solution of the LQG control problem; see [40] for a more detailed derivation. The essential idea is to use the *dynamic programming* method based on the following *expected cost-to-go*:

$$J_t[u, z] = \mathbb{E} \left[\int_t^T \left(\pi(\hat{x}_s)^\top Q \pi(\hat{x}_s) + u_s^\top R u_s \right) ds \mid \pi(\hat{x}_t) = z \right].$$

The goal is to obtain the minimum of this function, i.e., $J_t^*(z) = \min_{u[t,T]} J_t[u, z]$, with respect to the input in the time interval $[t, T]$, denoted by $u[t, T]$. Now we rewrite $J_t^*(z)$ in the following form:

$$\begin{aligned} J_t^*(z) &= \min_{u[t,T]} \mathbb{E} \left[\int_t^{t+dt} \left(\pi(\hat{x}_s)^\top Q \pi(\hat{x}_s) + u_s^\top R u_s \right) ds \right. \\ &\quad \left. + \int_{t+dt}^T \left(\pi(\hat{x}_s)^\top Q \pi(\hat{x}_s) + u_s^\top R u_s \right) ds \mid \pi(\hat{x}_t) = z \right] \\ &= \min_{u_t} \left\{ (z^\top Q z + u_t^\top R u_t) dt + J_{t+dt}^*(z + dz) \right\}. \end{aligned}$$

Then, noting that $\pi(\hat{x}_t)$ obeys Eq. (7) and $d\bar{w}_t = dy_t - C\pi(\hat{x}_t)dt$ is the standard classical Wiener process satisfying $d\bar{w}_t d\bar{w}_t^\top = D\Theta D^\top dt$, we see that the optimal value function $J_t^*(z)$ satisfies the *Bellman equation*

$$\begin{aligned} \min_{u_t} \left\{ \left\| u_t + \frac{1}{2} R^{-1} F^\top \frac{\partial J_t^*(z)}{\partial z} \right\|_R^2 - \frac{1}{4} \left(\frac{\partial J_t^*(z)}{\partial z} \right)^\top F R^{-1} F^\top \frac{\partial J_t^*(z)}{\partial z} + \frac{\partial J_t^*(z)}{\partial t} \right. \\ \left. + z^\top Q z + \left(\frac{\partial J_t^*(z)}{\partial z} \right)^\top A z + \frac{1}{2} \text{Tr} \left[\frac{\partial^2 J_t^*(z)}{\partial z^2} K_t D \Re(\Theta) D^\top K_t^\top \right] \right\} = 0, \end{aligned}$$

with the terminal condition $J_T^*(z) = 0$. Here we have defined $\|x\|_R^2 = x^\top R x$. The optimal control input is thus given by

$$u_t^* = -\frac{1}{2} R^{-1} F^\top \frac{\partial J_t^*(z)}{\partial z}. \quad (27)$$

The optimal value function $J_t^*(z)$ is then determined from the following partial differential equation:

$$\begin{aligned} \frac{\partial J_t^*(z)}{\partial t} + z^\top Q z - \frac{1}{4} \left(\frac{\partial J_t^*(z)}{\partial z} \right)^\top F R^{-1} F^\top \frac{\partial J_t^*(z)}{\partial z} + \left(\frac{\partial J_t^*(z)}{\partial z} \right)^\top A z \\ + \frac{1}{2} \text{Tr} \left[\frac{\partial^2 J_t^*(z)}{\partial z^2} K_t D \Re(\Theta) D^\top K_t^\top \right] = 0. \end{aligned}$$

Now we assume that the solution is of the quadratic form $J_t^*(z) = z^\top P_t z + \nu_t$ with $P_t \in \mathbb{R}^{2n \times 2n}$ and $\nu_t \in \mathbb{R}$; then the above partial differential equation is reduced to

$$\begin{aligned} z^\top \left(\dot{P}_t + P_t A + A^\top P_t - P_t F R^{-1} F^\top P_t + Q \right) z \\ + \dot{\nu}_t + \text{Tr} [P_t K_t D \Re(\Theta) D^\top K_t^\top] = 0. \end{aligned}$$

This equality must hold for any $z \in \mathbb{R}^{2n}$, and we thus obtain the following set of ordinary differential equations:

$$\dot{P}_t + P_t A + A^\top P_t - P_t F R^{-1} F^\top P_t + Q = 0, \quad \dot{\nu}_t + \text{Tr} [P_t K_t D \Re(\Theta) D^\top K_t^\top] = 0.$$

It follows from $J_T^*(z) = 0$ that the terminal conditions are $P_T = 0$ and $\nu_T = 0$. Under the assumption that the above set of equations have solutions, the optimal controller (27) is given by

$$u_t^* = -R^{-1} F^\top P_t \pi(\hat{x}_t). \quad (28)$$

Moreover, we now have

$$\langle J_0^*(\hat{x}_0) \rangle = \langle \hat{x}_0^\top P_0 \hat{x}_0 + \nu_0 \rangle = \langle \hat{x}_0^\top P_0 \hat{x}_0 \rangle + \int_0^T \text{Tr} [P_t K_t D \Re(\Theta) D^\top K_t^\top] dt,$$

hence the minimum of the original cost function (13) is given by

$$J[u^*] = \lim_{T \rightarrow \infty} \frac{1}{T} \langle J_0^*(\hat{x}_0) \rangle + \text{Tr}(Q V_\infty) = \text{Tr} [P_\infty K_\infty D \Re(\Theta) D^\top K_\infty^\top] + \text{Tr}(Q V_\infty).$$

Appendix B: Condition for the cheap control [30, 31, 32]

Let us consider the system whose transfer function matrix is given by $\Xi(s) = \bar{Q}(sI - A)^{-1}F$, which we simply call the system (A, F, \bar{Q}) . First, if there exist a complex number $z \in \mathbb{C}$ and a vector u such that $u^\top G(z) = 0$ or $G(z)u = 0$, then z is called a *zero* (more precisely, it is called a transmission zero). Then the system (A, F, \bar{Q}) is called *minimum phase*, if all the zeros of $\Xi(s)$ have negative real part. Next the system (A, F, \bar{Q}) is called *right invertible*, if $\Xi(s)$ has full row rank for at least one $s \in \mathbb{C}$. In general, such a minimum phase and right invertible system is regarded as a system easy to control; an intuitive understanding of this fact is that there exists an “inverse” and “stable” system (i.e., there exists $\Xi(s)^{-1}$ and all its poles have negative real part), and this system completely compensates $\Xi(s)$. In fact, as mentioned in Section 2.4, for such a system there exists a stabilizing controller that well suppresses the dynamical fluctuation of the (estimated) system variables.

Here we prove that the opto-mechanical system examined in Section 4 actually satisfies the above condition for cheap control. Note that the LQG problem is now formulated with the choice

$$\bar{Q} = \begin{bmatrix} 1 & 0 & 0 & 0 \\ 0 & 1 & 0 & 0 \end{bmatrix},$$

which actually yields $Q = \bar{Q}^\top \bar{Q} = \text{diag}\{1, 1, 0, 0\}$; see Eq. (22). The F matrix representing the actuator mechanism of the controller can be typically chosen as follows. First, if the oscillator can be directly manipulated via a piezo electrical device, then $F_1 = [0, 1, 0, 0]^\top$, meaning that the momentum of the oscillator can be driven by an external force. Another typical setup for actuation is that the control is carried out by modulating the input probe field, in which case $F_2 = [0, 0, 1, 0]^\top$, where especially only the \hat{q}_2 quadrature is assumed to be modulated (it can be proven that modulating \hat{p}_2 does not affect on the condition to be fulfilled). Then we have

$$\begin{aligned} \Xi_1(s) &= \bar{Q}(sI - A)^{-1}F_1 = \frac{1}{(s + \kappa/2)^2 + \omega^2} \begin{bmatrix} \omega \\ s + \gamma/2 \end{bmatrix}, \\ \Xi_2(s) &= \bar{Q}(sI - A)^{-1}F_2 = \frac{\lambda}{[(s + \kappa/2)^2 + \omega^2](s + \kappa/2)} \begin{bmatrix} \omega \\ s + \gamma/2 \end{bmatrix}. \end{aligned}$$

Therefore, in both cases, the system (A, F, \bar{Q}) is minimum phase and right invertible.

Appendix C: Logarithmic negativity

For a two-mode Gaussian state with mean zero, its correlation property can be completely characterized by the covariance matrix

$$V = \begin{bmatrix} V_1 & V_2 \\ V_2^\top & V_3 \end{bmatrix}, \quad (29)$$

where V_i are 2×2 matrices. In particular, the following *logarithmic negativity* [46, 47] can be used as a reasonable measure of entanglement of this Gaussian state:

$$E_{\mathcal{N}} = \max\{0, -\log(2\nu)\},$$

where $\log x$ denotes the natural logarithm of x , and

$$\nu = \frac{1}{\sqrt{2}} \sqrt{\tilde{\Delta} - \sqrt{\tilde{\Delta}^2 - 4\det(V)}}, \quad \tilde{\Delta} = \det(V_1) + \det(V_3) - 2\det(V_2).$$

Actually the state is entangled if and only if $E_{\mathcal{N}} > 0$.

In our case, the output of BS1 is an entangled Gaussian field; particularly when $\theta = \pi/2$, the covariance (more precisely the spectral density) matrix is given by Eq. (29) with

$$\begin{aligned} V_1 &= \text{diag}\{\alpha_1^2 e^r + \beta_1^2, \alpha_1^2 e^{-r} + \beta_1^2\}/2, \\ V_2 &= \text{diag}\{\alpha_1 \beta_1 (1 - e^r), \alpha_1 \beta_1 (1 - e^{-r})\}/2, \\ V_3 &= \text{diag}\{\beta_1^2 e^r + \alpha_1^2, \beta_1^2 e^{-r} + \alpha_1^2\}/2. \end{aligned}$$

This yields $\nu = \sqrt{d - \sqrt{d^2 - 1}}/2$ with $d = 2\alpha_1^2\beta_1^2(e^r + e^{-r} - 2) + 1$, and thus $E_{\mathcal{N}} > 0$ for all $\beta_1 \in (0, 1)$ and $r \neq 0$. Note that, hence, the maximal entangled field for $\theta = \pi/2$ is produced when $\alpha_1^2 = \beta_1^2 = 1/2$.

References

- [1] A. Einstein, B. Podolsky, and N. Rosen, Can quantum-mechanical description of physical reality be considered complete? *Phys. Rev.* **47**, 777 (1935).
- [2] M. A. Nielsen and I. L. Chuang, *Quantum Computation and Quantum Information* (Cambridge Univ. Press, 2000).
- [3] J. P. Dowling and G. J. Milburn, Quantum technology: the second quantum revolution, *Phil. Trans. R. Soc. Lond. A* **361**, 1655/1674 (2003).
- [4] S. L. Braunstein and C. M. Caves, Statistical distance and the geometry of quantum states, *Phys. Rev. Lett.* **72**, 3439 (1994).
- [5] V. Giovannetti, S. Lloyd, and L. Maccone, Quantum-enhanced measurements: Beating the standard quantum limit, *Science* **306**, 1330 (2004).
- [6] M. W. Mitchell, J. S. Lundeen, and A. M. Steinberg, Super-resolving phase measurements with a multi-photon entangled state, *Nature* **429**, 161/164 (2004).
- [7] T. Nagata, R. Okamoto, J. L. O'Brien, K. Sasaki, and S. Takeuchi, Beating the standard quantum limit with four-entangled photons, *Science* **316**, 726/729 (2007).
- [8] L. Appel, P. J. Windpassinger, D. Oblak, H. U. Busk, N. Kjargaard, and E. S. Polzik, Mesoscopic atomic entanglement for precision measurements beyond the standard quantum limit, *P. Natl. Acad. Sci.* **106**, 10960/10965 (2009).
- [9] A. L.-Chauvet, J. Appel, J.J. Renema, D. Oblak, N. Kjargaard, and E. S. Polzik, Entanglement-assisted atomic clock beyond the projection noise limit, *New. J. Phys.* **12-6**, 065032 (2010).
- [10] H. J. Kimble, Y. Levin, A. B. Matsko, K. S. Thorne, S. P. Vyatchanin, Conversion of conventional gravitational-wave interferometers into quantum nondemolition interferometers by modifying their input and/or output optics, *Phys. Rev. D* **65**, 022002 (2001).
- [11] J. Aasi, et. al., Enhanced sensitivity of the LIGO gravitational wave detector by using squeezed states of light, *Nature Photonics* **7**, 613 (2013).
- [12] K. Iwasawa, K. Makino, H. Yonezawa, M. Tsang, A. Davidovic, E. Huntington, and A. Furusawa, Quantum-limited mirror-motion estimation, *Phys. Rev. Lett.* **111**, 163602 (2013).
- [13] C. Schafermeier, et. al., Quantum enhanced feedback cooling of a mechanical oscillator using non-classical light, *Nature Comm.* **7**, 13628 (2016)
- [14] S. P. Vyatchanin and E. A. Zubova, Quantum variation measurement of a force, *Phys. Lett. A* **201**, 269/274 (1995).
- [15] H. M. Wiseman and G. J. Milburn, *Quantum Measurement and Control* (Cambridge Univ. Press, 2009).
- [16] K. Jacobs, *Quantum Measurement Theory and its Applications* (Cambridge Univ. Press, 2014).
- [17] V. P. Belavkin, Measurement, filtering and control in quantum open dynamical systems, *Rep. on Math. Phys.* **43**, 405/425 (1999).
- [18] L. Bouten, R. van Handel, and M. James, An introduction to quantum filtering, *SIAM J. Control Optim.* **46**, 2199/2241 (2007).

- [19] M. G. Genoni, S. Mancini, H. M. Wiseman, and A. Serafini, Quantum filtering of a thermal master equation with purified reservoir, *Phys. Rev. A* **90**, 063826 (2014).
- [20] H. A. Bachor and T. C. Ralph, *A Guide to Experiments in Quantum Optics* (Weinheim, Wiley-VCH, 2004).
- [21] M. R. James, H. I. Nurdin, and I. R. Petersen, H^∞ control of linear quantum stochastic systems, *IEEE Trans. Automat. Contr.* **53**-8, 1787/1803 (2008).
- [22] H. I. Nurdin, M. R. James, and I. R. Petersen, Coherent quantum LQG control, *Automatica* **45**, 1837 (2009).
- [23] R. Hamerly and H. Mabuchi, Advantages of coherent feedback for cooling quantum oscillators, *Phys. Rev. Lett.* **109**, 173602 (2012).
- [24] N. Yamamoto, Coherent versus measurement feedback: Linear systems theory for quantum information, *Phys. Rev. X* **4**, 041029 (2014).
- [25] N. Yamamoto, Quantum feedback amplification, *Phys. Rev. Applied* **5**, 044012 (2016).
- [26] A. Furusawa and P. van Loock, *Quantum Teleportation and Entanglement: A Hybrid Approach to Optical Quantum Information Processing* (Berlin: Wiley-VCH, 2011).
- [27] A. C. Doherty, S. M. Tan, A. S. Parkins, and D. F. Walls, State determination in continuous measurement, *Phys. Rev. A* **60**, 2380 (1999).
- [28] A. C. Doherty and K. Jacobs, Feedback control of quantum systems using continuous state estimation, *Phys. Rev. A* **60**, 2700 (1999).
- [29] V. P. Belavkin and S. C. Edwards, Quantum filtering and optimal control, in *Quantum Stochastics and Information: Statistics, Filtering and Control*, 143/205 (World Scientific, 2008).
- [30] H. Kwakernaak and R. Sivan, The maximal achievable accuracy of linear optimal regulators and linear optimal filters, *IEEE Trans. Automat. Contr.* **17**, 79/86 (1972).
- [31] M. M. Seron, J. Braslavsky, and G. Goodwin, *Fundamental Limitations in Filtering and Control* (New York: Springer-Verlag, 1997).
- [32] M. M. Seron, J. H. Braslavsky, P. V. Kokotovic, and D. Q. Mayne, Feedback limitations in nonlinear systems: From Bode integrals to cheap control, *IEEE Trans. Automat. Contr.* **44**-4, 829/833 (1999).
- [33] S. Mancini, D. Vitali, and P. Tombesi, Optomechanical cooling of a macroscopic oscillator by homodyne feedback, *Phys. Rev. Lett.* **80**, 688 (1998).
- [34] A. Hopkins, K. Jacobs, S. Habib, and K. Schwab, Feedback cooling of a nanomechanical resonator, *Phys. Rev. B* **68**, 235328 (2003).
- [35] R. Hamerly and H. Mabuchi, Coherent controllers for optical-feedback cooling of quantum oscillators, *Phys. Rev. A* **87**, 013815 (2013).
- [36] S. G. Hofer and K. Hammerer, Entanglement-enhanced time-continuous quantum control in optomechanics, *Phys. Rev. A* **91**, 033822 (2015).
- [37] D. J. Wilson, V. Sudhir, N. Piro, R. Schilling, A. Ghadimi, and T. J. Kippenberg, Measurement-based control of a mechanical oscillator at its thermal decoherence rate, *Nature* **524**, 325 (2015).
- [38] W. Wieczorek, S. G. Hofer, J. Hoelscher-Obermaier, R. Riedinger, K. Hammerer, and M. Aspelmeyer, Optimal state estimation for cavity optomechanical systems, *Phys. Rev. Lett.* **114**, 223601 (2015).
- [39] V. Kucera, A contribution to matrix quadratic equation, *IEEE Trans. Automat. Contr.* **17**-3, 344/347 (1972).

- [40] A. Bensoussan, *Stochastic Control of Partially Observable Systems* (Cambridge University Press, 1992).
- [41] L. Bouten and R. van Handel, On the separation principle of quantum control, in *Quantum Stochastics and Information: Statistics, Filtering and Control*, 206/238 (World Scientific, 2008).
- [42] S. S. Szigeti, A. R. R. Carvalho, J. G. Morley, and M. R. Hush, Ignorance is bliss: General and robust cancellation of decoherence via no-knowledge quantum feedback, *Phys. Rev. Lett.* **113**, 020407 (2014).
- [43] G. J. Milburn and M. J. Woolley, An introduction to quantum optomechanics, *acta physica slovacica* **61-5**, 483/601 (2011).
- [44] M. Poggio, C. L. Degen, H. J. Mamin, and D. Rugar, Feedback cooling of a cantilever's fundamental mode below 5 mK, *Phys. Rev. Lett.* **99**, 017201 (2007).
- [45] N. Didier, A. Kamal, W. D. Oliver, A. Blais, and A. A. Clerk, Heisenberg-limited qubit read-out with two-mode squeezed light, *Phys. Rev. Lett.* **115**, 093604 (2015).
- [46] G. Vidal and R. F. Werner, Computable measure of entanglement, *Phys. Rev. A* **65**, 032314 (2002).
- [47] M. B. Plenio, The logarithmic negativity: A full entanglement monotone that is not convex, *Phys. Rev. Lett.* **95**, 090503 (2005).